Icarus 280 (2016) 199–204

Contents lists available at ScienceDirect

Icarus

journal homepage: www.elsevier.com/locate/icarus

The first long-term all-sky imager observation of lunar sodium tail

Masaki N. Nishino*, Kazuo Shiokawa, Yuichi Otsuka

Institute for Space-Earth Environmental Research, Nagoya University, Furocho, Chikusa-ku, Aichi, 464-8601, Japan

ARTICLE INFO

Article history:
Received 25 March 2016
Revised 11 July 2016
Accepted 1 August 2016
Available online 4 August 2016

Keywords:
Moon
Moon surface
Solar wind

ABSTRACT

The Moon possesses a long tail of neutral sodium atoms that are emitted from the lunar surface and transported anti-sunward by the solar radiation pressure. Since the earth crosses the lunar sodium tail for a few days around the new moon, the resonant light emission from sodium atoms can be detected from the ground. Here we show the first long-term (16 years) observation of the lunar sodium tail, using an all-sky imager at Shigaraki Observatory (35°N, 136°E), Japan. We have surveyed our database of all-sky sodium images at a wavelength of 589.3 nm to find more than 20 events in which a bright spot emerges around the anti-lunar point during the new moon periods. We could not find any clear correlation between the sodium brightness and solar wind parameters (density, speed, dynamic pressure, and F10.7 index). In particular, no enhancement of the sodium spot brightness is detected even under very high density solar wind conditions (70 cm^{-3}; an order-of-magnitude higher than usual), which means that solar wind sputtering is not a principal mechanism of the formation of the lunar sodium tail.

1. Introduction

The tenuous sodium and potassium exosphere of the Earth's Moon has been previously discovered (Potter and Morgan, 1988; Tyler et al., 1988). The generation mechanism of the sodium exosphere is one of unrevealed problems of lunar sciences. Candidates for the mechanism of sodium emission from the planetary surface are (1) solar wind sputtering, (2) photon-stimulated desorption (PSD), (3) micrometeoroid impact, and (4) thermal desorption. In the Moon's case, the first three mechanisms are candidates for the sodium exosphere formation.

The fate of the sodium atoms emitted from the lunar surface depends on its initial speed and the ambient environment including the solar radiation. Some fraction of the sodium atoms escapes from the gravity sphere of the Moon and then accelerated by the solar radiation pressure to form a tail-like structure. The lunar sodium tail was first discovered by a ground-based observation during the Leonid meteor shower (Smith et al., 1999). Sodium atoms emitted from the lunar surface by the meteor impact are accelerated to the anti-sunward direction by the solar radiation pressure to form the lunar sodium tail. Light emission from sodium atoms by the resonant light scattering by solar light can be detected around the new Moon period when the Earth is enveloped by the lunar sodium tail formed by the Leonid meteor shower.

On the other hand, the lunar sodium tail was observed not only under the Leonid meteor shower but also during non-meteor periods (Shiokawa et al., 2000). This fact does not deny possible bursty sodium emission by meteor shower, but it suggests stationary emission of sodium atoms from the lunar surface to form the exosphere. However, a previous statistical study using all-sky images between 2006–2008 reported that the sodium tail brightness has no correlation with sporadic and shower meteor activity, solar wind proton energy flux and solar near ultra violet (NUV) patterns (Matta et al., 2009).

In this study, we use the first long-term data from an all-sky camera between 2000–2015 (16 years) to study relation between the solar wind parameters and the sodium tail brightness.

2. Instrumentation

We use sodium-band all-sky images obtained at the Shigaraki observatory (35°N, 136°E) in Japan. The camera is a part of the Optical Mesosphere Thermosphere Imagers (OMTI) (see Shiokawa et al., 1999 in detail). The wavelength and the bandwidth of the camera is 589.3 nm and 1.83 nm, respectively. The sodium-band images are taken every 30 min with an exposure time of 105 s. Because the sensor is optimised to observe the weak night airglow, the camera is in operation only when the Sun and the Moon are invisible. The Doppler shift of the sodium emission line is negligible in this study, for the anti-sunward speed of the sodium atoms by the solar radiation pressure is estimated to be several tens km/s at most (Lee et al., 2011; Line et al., 2012) and thus Doppler-shifted emission lines are small enough to stay in the band width.

* Corresponding author. Fax: +81-527476323.
E-mail address: mnishino@isee.nagoya-u.ac.jp (M.N. Nishino).

http://dx.doi.org/10.1016/j.icarus.2016.08.004
0019-1035/

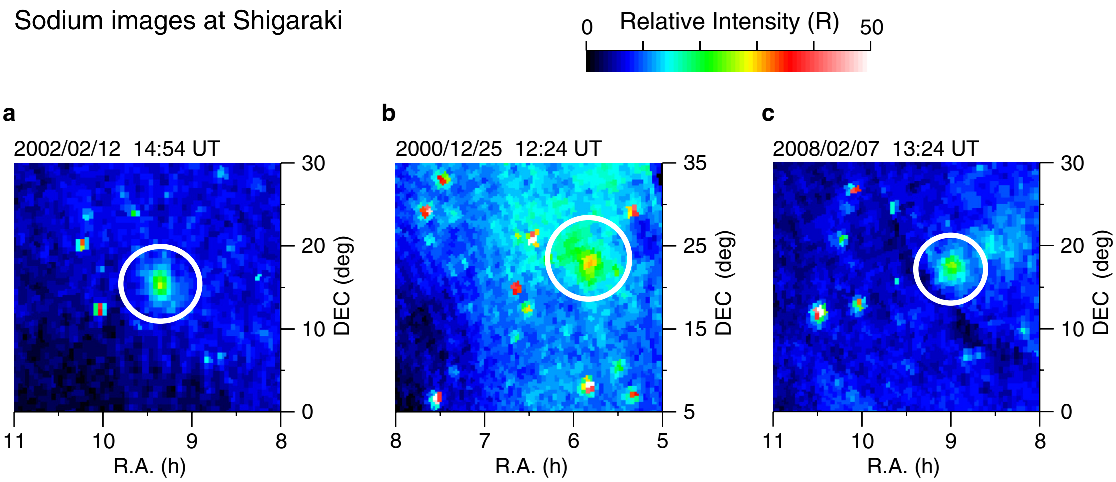

Fig. 1. Typical images of the lunar sodium spot obtained at (a) 14:54 UT on 12 February 2002, (b) 12:24 UT on 25 December 2000, and (c) 13:24 UT on 7 February 2008. The bright spot of the lunar sodium tail is pointed out by a white circle in each image. Other bright spots are stars and planets. (The brightest point (>50 *R*) in the 7 February 2008 image is the Saturn situated in the region of the Lion constellation.).

Table 1
List of sodium tail events at Shigaraki Observatory used in this study.

Date	Time (UT)	Brightness (R)	Nsw (cm^{-3})	Vsw ($km\ s^{-1}$)	Pdyn (nPa)	f10.7 (sfu)
2000/12/25	14:24	23	15.3	307	2.5	184
2001/12/14	14:19	14	9.9	346	2.3	223
2002/02/12	14:54	20	5.2	441	2.1	204
2003/12/23	14:44	15	9.9	493	4.4	128
2004/01/21	15:04	21	3.2	594	2.3	125
2004/02/20	14:34	14	0.7	442	0.29	97
2005/01/10	14:10	23	15.5	527	9.4	84
2007/12/09	13:04	17	6.1	332	1.15	78
2008/01/08	14:24	16	4.3	630	3.5	77
2008/02/07	13:24	18	2.0	499	0.89	69
2008/03/07	14:44	17	4.6	407	1.6	68
2008/12/27	14:44	23	3.9	430	1.3	67
2010/01/15	14:04	23	4.6	439	1.7	89
2010/12/05	14:04	12	10.4	307	1.7	84
2011/01/04	14:24	24	9.9	326	1.8	88
2011/02/03	14:14	15	24.8	326	4.1	78
2011/04/03	14:04	12	2.7	336	0.61	111
2014/01/01	15:24	16	3.0	337	0.69	136
2014/11/22	14:14	11	6.0	400	2.0	165
2015/01/20	14:04	19	5.8	339	1.3	120

After obtaining each sodium image, a limited area around the anti-lunar point is picked out to find a bright spot of the lunar sodium tail (See Fig. 1). Stronger emissions from the sodium layer in the Earth's mesosphere are treated as background and subtracted from each cut-out image. The determination error of the background sodium brightness in each cut-out image is about 5 R at most, which does not affect the results. Random noise in the CCD counts in each bin of the figures is estimated to be ∼ 0.3 R, which is much smaller than the determination error of the background sodium brightness.

In this study we use images obtained after 12 December 2000 when the all-sky camera was calibrated. All images in this paper are presented in the orthogonal coordinate system of the right ascension (RA) and declination (Dec).

The OMNI solar wind data are provided via CDAWeb. The OMNI data for the period of our interest are from ACE and Wind spacecraft.

3. Case studies

First we present 3 typical time series data to examine temporal variations of the sodium spot brightness in each new moon period.

We focus on a series of all-sky images obtained during a few days around new Moon at 07:41 UT on 12 February 2002. For the three days between 11 and 13 February, we obtain 66 all-sky images in the sodium band. We can determine the brightness of the sodium spot in 7 of 66 images.

The maximum brightness of the sodium spot for the 3 days is 20 R, which is detected at 14:54 UT on 12 February 2002 (i.e. 7.2 hours after the new Moon) (Fig. 1a). The peak of the lunar sodium spot exists at (RA, Dec) = (9.4 hr, 15°), which is close to the anti-lunar point at new Moon ((RA, Dec) = (9.80 hr, 17.77°)). Through the 3 days the lunar tail spot gradually drifts eastward (leftward in the image) by ∼ 3–4° a day (data not shown), which is consistent with previous studies (Line et al., 2012; Smith et al., 1999). The lunar sodium spot is the brightest on 12 February, while less brighter spots can be found on the previous and next days of the new Moon day (Fig. 2d). This trend is consistent with a previous study (Line et al., 2012). The solar wind parameters are in the typical ranges around the new Moon day (Fig. 2a–c). See also Table 1 for averages solar wind parameters.

Similar temporal variations around new Moon are observed in other 2 new Moon events of 25 December 2000 (Fig. 1b and 3) and 7 February 2008 (Fig. 1c and 4). In both events the sodium spot